

AIAA 81-0287R

Aerodynamic Properties of an Advanced Indirect Fire System (AIFS) Projectile

Martin R. Fink*

Norden Systems, Inc., Norwalk, Conn.

A wind-tunnel model of an advanced indirect fire system (AIFS) projectile was tested at Mach numbers of 1.5-2.2. This cannon-launched projectile has solid-fuel ramjet propulsion and folding aft fins. Its terminal maneuver configuration has a blunt seeker nose and deflectable canards. Upwash induced by body vortices at the small-span aft fins caused a nonlinear increase of static stability at greater than 3 deg angle of attack. This effort is not predicted by the commonly used design procedure of NACA Report 1307. It occurred for both the sharp-nosed powered flight and blunt-nosed terminal maneuver configurations. Increased static stability and the negative contribution of blunt-nose axial force to lift decreased the trimmed lift coefficient below that predicted at maximum canard deflection.

Introduction

EFFECTIVENESS of artillery against armored targets can be improved by replacing unguided shells with terminally guided, aerodynamically maneuverable projectiles. If targets are sufficiently near the battle area, they can be illuminated with lasers operated by forward observers and attacked by projectiles¹ that home in on the reflected energy. For targets that are more distant, each projectile must carry its own target identification system. The greater uncertainty about the target position at these longer ranges (indirect fire) requires that the projectile be capable of maneuvering to reach a target within a larger footprint area. The kinetic energy needed for such maneuvers can exceed that of an artillery projectile decelerated by aerodynamic drag. This is particularly true if the projectile has a blunt nose as needed by the target-detection seeker.

Aerodynamic considerations for an advanced indirect fire system (AIFS) are discussed. The system is advanced in that it uses a self-contained fire-and-forget terminal guidance system. A maximum range about twice that for conventional artillery shells is achieved by use of a solid-fuel ramjet to overcome aerodynamic drag prior to the terminal phase of flight. During powered flight, the ramjet axisymmetric inlet spike provides a low-drag aerodynamic shield for the blunt seeker dome. Natural variation of inlet mass flow rate with altitude is such that if thrust is nearly equal to zero-lift drag at sea level, they remain closely matched throughout a ballistic trajectory. Ramjet thrust is controlled by inlet air bleed ahead of the combustor to maintain zero axial acceleration. The trajectory closely approximates that for a projectile moving through a vacuum in the same gravitational field with the same initial velocity and direction. Effects of winds and of nonstandard atmospheric properties are greatly reduced by this easily implemented thrust control.

When sufficiently near the target, as determined by a timer, the inlet duct is closed to terminate thrust. The inlet spike then is removed to uncover the seeker dome and the canards are extended. The projectile is changed from a nonmaneuvering, zero net axial force device to a maneuverable but relatively high-drag configuration moving at close to the gun muzzle velocity. Several aerodynamic compromises are required between the behavior of the projectile within the gun tube, during ramjet powered flight and during the terminal maneuver. These are discussed herein.

Basic Concepts of AIFS

Projectile ranges of tactical interest could be obtained with cannon launch and either rocket or ramjet propulsion. An efficient rocket-assisted projectile would have a short burn time relative to the flight time. Its trajectory must be lofted to allow flight at higher altitudes with reduced aerodynamic drag, so the flight time would be long. In contrast, a ramjet vehicle would be most efficient if it were powered throughout its flight. The trajectory could approximate the minimum-flight-time vacuum trajectory corresponding to the range and launch velocity. For the 203 mm (8 in.) howitzer considered, the high specific impulse of a solid-fuel ramjet relative to a solid-propellant rocket causes the ramjet projectile to have less total weight. Because it also has shorter flight time and far more growth potential, ramjet propulsion was chosen.

As sketched in Fig. 1, the ramjet-powered AIFS has an axisymmetric spike inlet and annular cowl and duct surrounding the seeker, control actuators, and warhead. The ramjet combustion chamber, mixing chamber, and exhaust nozzle occupy the aft half of the projectile. Total length is about twice that of a conventional artillery shell and is limited by the loading mechanism. Volume would not be available for placing high-aspect-ratio lifting surfaces within the projectile body and deploying them like jackknife blades.² Thus the main lifting surfaces are constrained to be small-span, low-aspect-ratio panels folded against a reduced-diameter portion of the body.

Conventional artillery shells have a closed base. The gun gas pressure acts against the base and against the rotating band (obturator) that provides a seal between the projectile and gun barrel to accelerate the shell. If this structural design (Fig. 2a) was used for a long slender ramjet, its combustion chamber walls would have to be much heavier than is needed to withstand the relatively low combustion pressure. If the ramjet exhaust nozzle is open and the port in the combustion chamber dome is closed, but the obturator remains near the

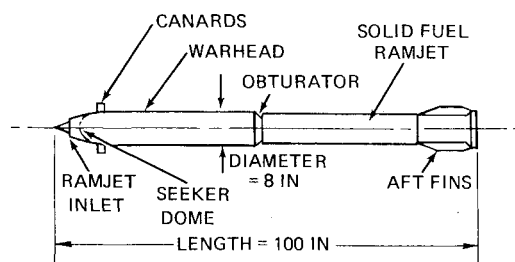


Fig. 1 General view of AIFS projectile.

Presented as Paper 81-0287 at the AIAA 19th Aerospace Sciences Meeting, St. Louis, Mo., Jan. 12-15, 1981; submitted Feb. 27, 1981; revision received Aug. 27, 1981. Copyright © American Institute of Aeronautics and Astronautics, Inc., 1981. All rights reserved.

*Chief of Aerodynamics, Associate Fellow AIAA.

base (Fig. 2b), the combustion chamber walls must withstand the gun breech pressure. This also produces a heavy design.

In the approach chosen (Fig. 2c), the diameter of the combustion chamber is reduced and the obturator is placed near midlength. The exhaust nozzle is open and the combustion chamber dome port is closed. A segmented centering band (bourrelet), with openings to allow the gun gases to flow through, prevents pitch and yaw motion of the projectile within the tube. Dimensions of the exhaust nozzle, centering-band nozzles, combustion chamber, and annulus between the projectile and tube are carefully matched. Shock waves and gun gas flows produced when the gun is fired cause transient pressure differences radially across the combustion chamber walls and axially across the nozzle. For a properly matched design, these pressure differences are much smaller than the gun breech pressure. The gun gas pressure is imposed against the combustion chamber dome and against the obturator which presses against a projectile structure mounted on that dome. Thus the ramjet combustion chamber and its nozzle and solid fuel are pulled through the gun tube. Only the warhead, guidance and control, and inlet duct are subjected to compressive buckling loads. Small-span aft fins are folded into the space between the combustion chamber outer wall and the gun tube, and dimensions must be adjusted for this additional blockage area.

After the projectile moves past the gun muzzle, the hot high-pressure gun gases contained within the combustion chamber flow out of the exhaust nozzle and produce additional thrust. The pressure in this chamber then decreases to less than that within the ramjet inlet duct. A port cover in the combustion chamber dome then is opened. The ramjet solid fuel has been preheated by the gun gases, and it ignites in the presence of the inlet air.

The aft fins must have a small enough exposed semispan to fit within the annulus determined from a balance of the propagating gun gas pressures. Also, they must be large enough to provide static stability at launch when the center of gravity is furthest aft. Note that use of a statically stable nonlifting projectile, and thrust approximately equal to drag, greatly reduces the effects of winds and atmospheric nonuniformity on the trajectory. Crosswinds cause the projectile to point into the relative wind, but the flight trajectory continues to closely approximate that of an unpowered vehicle in the absence of an atmosphere. Thus the position error at the start of the target-seeking terminal phase is greatly decreased. Static stability increases during the flight as the ramjet fuel, located aft of the center of gravity, is consumed.

Flights at less than maximum range are accomplished at a reduced gun elevation angle. Thus the trajectories are flown with smaller powered flight times, but lower average altitudes and thus higher average ramjet thrust. The amount of solid fuel burned, from launch to start of the target acquisition

phase of flight, varies only slightly with range. Projectile weight during the terminal maneuver and the maneuver acceleration achievable for a given velocity and control deflection are nearly the same for maximum and minimum range. This is an advantage of the chosen flight profile and the inherent behavior of a solid-fuel ramjet, as compared with cruise at constant altitude and velocity.

At a preset time corresponding to an appropriate altitude, the terminal maneuver is initiated by closing the port cover to terminate thrust, blowing off the ramjet inlet spike to provide an unobstructed view for the seeker, deploying the canards, and reducing the flight path descent angle. The seeker then scans through its field of view. When a target is located, canard control signals are developed to command a maneuver that will impact the projectile against the target. Intended targets are tanks and other armored vehicles, and the projectile contains a shaped-charge warhead.

Wind-Tunnel Tests

Wind-tunnel tests were conducted with an 0.35 scale model of the nominal 203 mm (8.00 in.) diam, 2.5 m (100 in.) length projectile. The model was tested in the 1.2×1.2 m (4×4 ft) supersonic test section of the Vought high-speed wind tunnel. Mach numbers were 1.5, 1.8, and 2.2 at a Reynolds number of 20×10^6 based on model length. This is about 1/3 to 1/5 the full-scale Reynolds numbers for this velocity range. Model components could be assembled to represent the powered-flight configuration with a faired sharp nose and aft fins, or the terminal maneuver configuration with a blunt nose, cruciform in-line canards, and aft fins. Sand grain roughness was placed at 10% chord on the canards and aft fins to assure boundary-layer transition.

Powered Flight Configuration

The projectile's center of gravity is furthest aft just after it leaves the gun barrel, before the ramjet fuel has ignited. Fins to stabilize the projectile must have a small enough span so that, when folded, they fit between the outer wall of the combustion chamber and the inner wall of the gun barrel. The combustion chamber wall diameter is sized by the projectile length that can be handled by available loading equipment and by the required ramjet thrust and burn time. It is also sized by the need to have only small differences between unsteady pressures inside and outside the chamber when the gun is fired. Combustion chamber diameter was locally reduced in the region occupied by the aft fins.

Both planar and wraparound cruciform aft fins with the same planform were tested on the wind-tunnel model. The ratio of local diameter to total span was 0.58, which is relatively large. Measured variations of pitching moment coefficient with angle of attack at a Mach number of 2.2 are

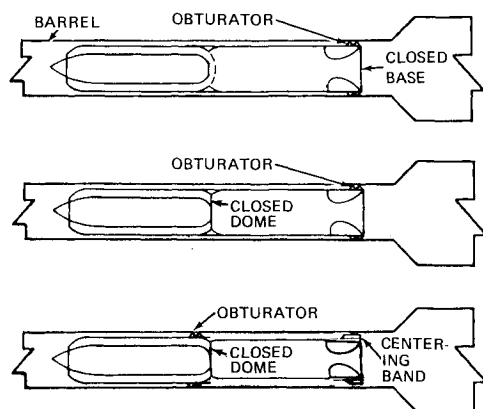


Fig. 2 Design concepts for withstanding gun gas pressure against the projectile.

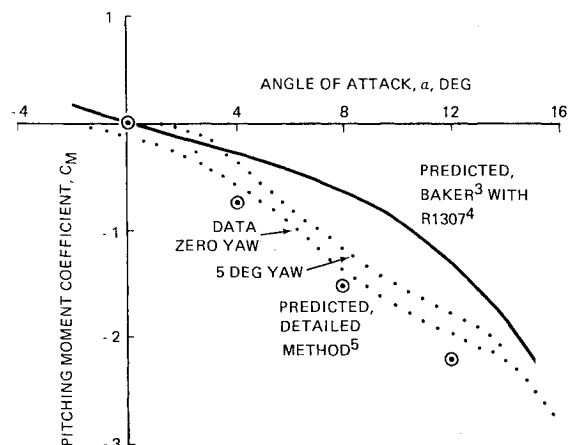


Fig. 3 Pitching moment coefficient for powered flight configuration at Mach 2.2.

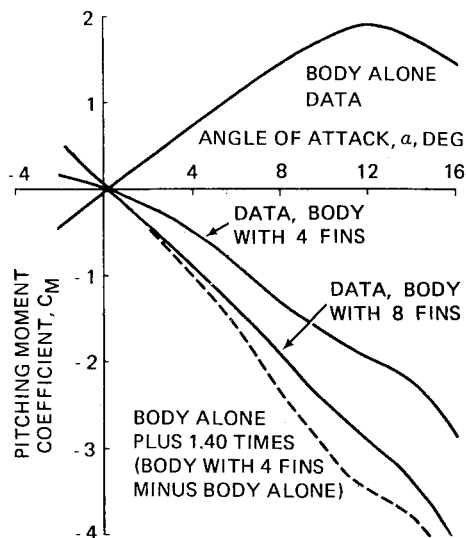


Fig. 4 Pitching moment coefficient for powered flight configuration with four or eight planar aft fins at Mach 2.2.

shown in Fig. 3. Instability of the body alone (not shown) was reduced by nonlinear crossflow effects. Measured moment was reasonably predicted by Baker's method.³ Both the planar and wraparound fins provided adequate static stability at small angles of attack, followed by increased static stability above a 3 deg angle. Use of the standard rapid-calculation NASA method⁴ for the fins and fin-body interactions, combined with Baker's method³ for the body, closely predicted the measured levels at small angles and above 15 deg angle. It failed to predict the increased negative levels at intermediate angles. Fin aspect ratio was below the minimum value for Baker's data correlation for body-tail configurations.³ That method (not shown) greatly overpredicted the measured normal force and pitching moment. A far more rigorous method⁵ requiring an order-of-magnitude greater computer run time was also used. That method predicted the measured nonlinear increase of stability and attributed it to the upwash induced by body vortices at the fins.

Data for the model at 45 deg roll angle essentially matched that for zero roll. However, data for 22.5 deg roll had a weaker nonlinear increase of stability. This result is consistent with the predicted flow process that causes the increase.

A possibility existed that early flight test vehicles, with thick combustion chamber walls, would have their center of gravity too far aft and would not be aerodynamically stable. The configuration had sufficient space for eight equally spaced folded aft fins. Doubling the number of fins does not double their contribution to lift and static stability. Pressure fields of adjacent fins are predicted to interfere with each other. For this diameter to span ratio, changing from four to eight fins was predicted⁶ to increase the contribution of the fins plus aft body by a factor of 1.4.

Measured variations of pitching moment coefficient with angle of attack at a Mach number of 2.2 are shown in Fig. 4 for the wind-tunnel model body alone and with four and eight planar aft fins. Also shown is the curve calculated by adding, to the body-alone data, 1.4 times the measured increment of pitching moment caused by four fins. This gives a good prediction of the eight-fin data for small and large angles of attack but overpredicts at moderate angles. Evidently the eight-fin configuration had a weaker interaction with the body vortices.

Terminal Maneuver Configuration

Measured variation of lift coefficient with angle of attack for the wind-tunnel model at zero canard deflection and a Mach number of 1.5 is shown in Fig. 5. The data were closely

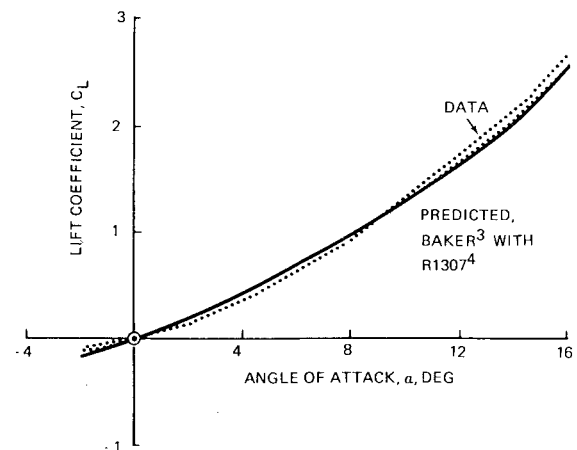


Fig. 5 Lift coefficient for terminal maneuver configuration with zero canard deflection at Mach 1.5.

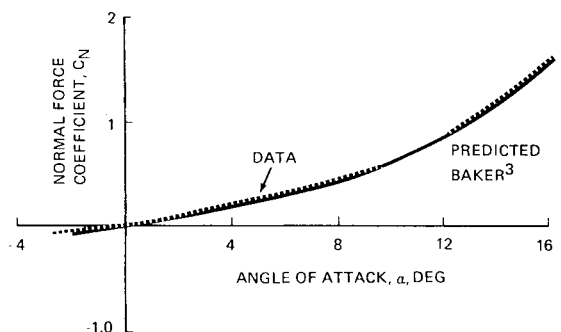


Fig. 6 Normal force coefficient for terminal maneuver blunt-nosed body alone at Mach 1.5.

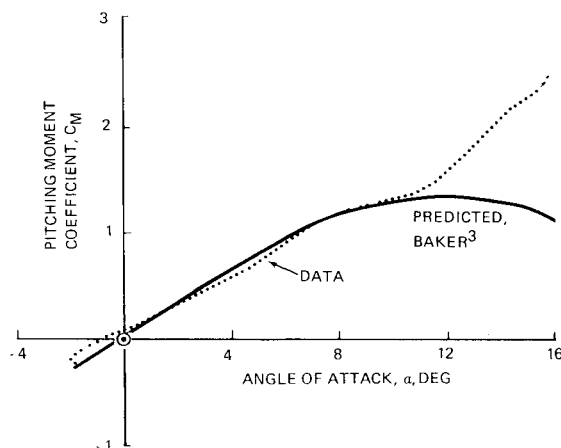


Fig. 7 Pitching moment coefficient for terminal maneuver blunt-nosed body alone at Mach 1.5.

predicted by a combination of the rapid-calculation methods for nonlinear lift of the body³ and lift of the lifting surfaces in the presence of a body.⁴ Interaction between the canard and the aft fin was predicted to be negligible beyond several degrees angle of attack. The projectile body is so long, relative to the canard and fin spans, that the canard wake tends to pass far above the aft fins. The previously cited rigorous aerodynamic prediction method⁵ is not applicable to this blunt-nosed configuration.

Close agreement between predicted and measured lift, shown in Fig. 5, proved to be a coincidental result of compensating errors. The largest error came from neglecting the negative contribution of axial force to the predicted lift

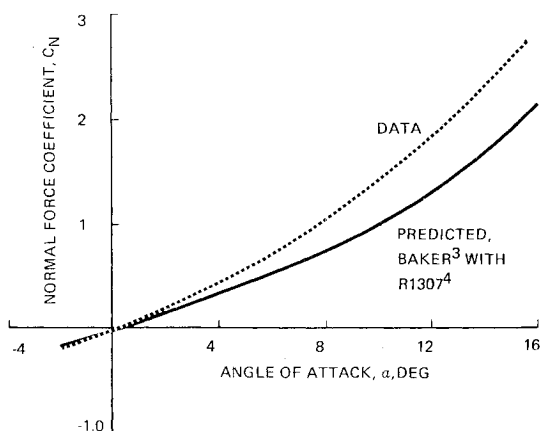


Fig. 8 Normal force coefficient for terminal maneuver blunt-nosed body plus aft fins at Mach 1.5.

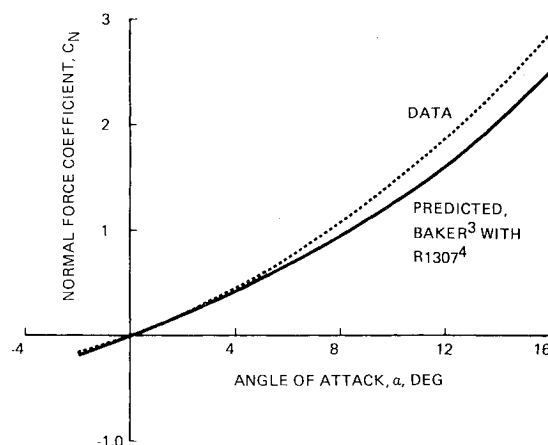


Fig. 10 Normal force coefficient for terminal maneuver configuration at Mach 1.5.

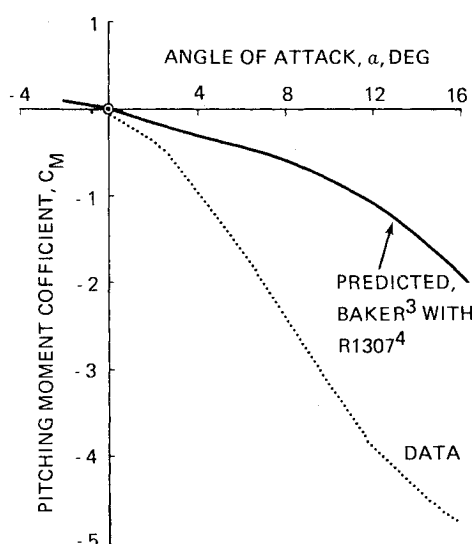


Fig. 9 Pitching moment coefficient for terminal maneuver blunt-nosed body plus aft fins at Mach 1.5

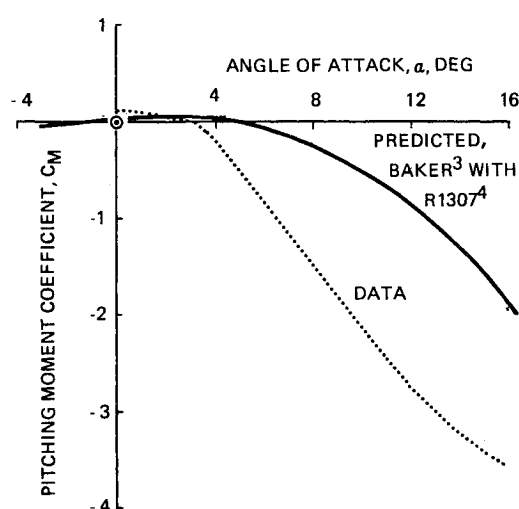


Fig. 11 Pitching moment coefficient for terminal maneuver configuration at Mach 1.5.

coefficient. This model had a very blunt seeker nose. The axial force coefficient was larger than one, so the predicted lift coefficient should have been decreased by more than the sine of the angle of attack. Even though the projectile is long and slender, its aerodynamic coefficients should have been calculated like those for a short blunt-nosed body.

Measured and predicted variations of normal force and pitching moment coefficients for the blunt-nosed body model alone are compared in Figs. 6 and 7. Normal force was closely predicted throughout the angle-of-attack range. In contrast, measured body pitching moment failed to show the predicted nonlinear reduction of instability at moderate incidence. This behavior had been predicted because the center of the body planform area is aft of the center-of-gravity position after all the fuel has been burned. Apparently the blunt nose induced an increased local loading on the portion of the cylindrical body immediately downstream. Such behavior has been previously observed for flat-faced cylinders.

Agreement between measured and predicted aerodynamic coefficients for the blunt-nosed body model with canards extended (not shown) was similar to that with canards retracted. The canards are small relative to the body. They were designed to reduce static stability caused by the forward shift of the center of gravity as the fuel is burned. Being small, they are easily packaged, extended, and actuated. Deflecting the canards provides significant changes in pitching moment but relatively little change in normal force.

Comparisons of measured and predicted coefficients for the blunt-nosed body model without canards but with the aft fins extended are shown in Figs. 8 and 9. Normal force coefficients were more negative than had been predicted, with an abrupt change of slope beyond 3 deg angle of attack. The nonlinear interaction of body vortices with the aft fins, previously discussed in connection with the powered flight configuration, was more severe with this blunt nose shape.

Measured and predicted normal force and pitching moment coefficients for the body-canard-fin wind-tunnel model are shown in Figs. 10 and 11. Normal force on the body and canards had been closely predicted but normal force from the aft fins in the presence of the body (Fig. 8) was underpredicted. This caused underprediction for the complete configuration as shown in Fig. 10. By coincidence, the axial force contribution to negative lift brought the resulting measured lift coefficients into close agreement with the values predicted from only the calculated normal force (Fig. 5). Pitching moment coefficients (Fig. 11) were considerably more stable than was predicted at greater than 2 deg angle of attack. Measured increments of pitching moment due to canard deflection generally matched the predictions. However, the trimmed angle of attack was approximately halved because of the increased static stability caused by interaction of the aft fins and the body vortices.

The predicted maneuver footprint area would be excessively reduced by the above limitation on the trimmed angle of

attack. Therefore, this limit must be changed. Reduction of the aft fin static stability by reducing that fin's span would cause an unacceptable decrease of stability in unpowered flight. Increasing the canard size to generate larger trimming moments would impose packaging problems for the larger canards, actuators, and compressed-gas power supply. The solution chosen was to use the best available aerodynamic analysis for prediction of body-fin interactions,⁵ even though that analysis applies only to sharp-nosed bodies. This computer program was applied in a systematic study of fin planform geometry effects at this diameter-to-span ratio. A revised fin planform has been selected that is predicted to produce the required level of static stability and be less influenced by body vortexes. Wind-tunnel tests will be conducted to validate the predicted behavior prior to full-scale flights in which canards will be deployed and actuated.

Conclusions

1) Airloads induced by body vortexes on aft fins can be important for projectiles with a fin total span not much larger than the body diameter.

2) The lift coefficient of a long slender projectile at moderate (10 deg) angles of attack can be significantly smaller than the normal force coefficient if the configuration has a high-drag blunt nose. This obvious effect is omitted in some commonly used methods for predicting missile and projectile lift and pitching moment coefficients.

Acknowledgment

This work was conducted under Contract DAAK 10-80-C-0114 with U.S. Army Armament Research and Development Command, Picatinny Arsenal, Dover, N.J.

References

- ¹Morrison, P.H. and Amberntson, D.S., "Guidance and Control of a Cannon-Launched Guided Projectile," *Journal of Spacecraft and Rockets*, Vol. 14, June 1977, pp. 328-334.
- ²Washington, W.D., Wittmeyer, R.E., and Appich, W.H. Jr., "Body Slot Effects on Wing-Body and Wing-Tail Interference of a Typical Cannon-Launched Guided Projectile," AIAA Paper 80-0260, Jan. 1980.
- ³Baker, W. B. Jr., "Aerodynamic Coefficient Prediction Technique for Finned Missiles at High Incidence," *Journal of Spacecraft and Rockets*, Vol. 15, Nov.-Dec. 1978, pp. 328-333.
- ⁴Pitts, W.C., Nielsen, J.N., and Kaattari, G.E., "Lift and Center of Pressure of Wing-Body-Tail Combinations at Subsonic, Transonic, and Supersonic Speeds," NACA Rept. 1307, 1957.
- ⁵Nielsen, J.N., Hensch, M.J., and Smith, C.A., "A Preliminary Method for Calculating the Aerodynamic Characteristics of Cruciform Missiles to High Angles of Attack Including Effects of Roll Angle and Control Deflections," Office of Naval Research Rept. ONR-CR215-226-4F, Nov. 1977.
- ⁶Miles, J.W., "On Interference Factors for Finned Bodies," *Journal of the Aeronautical Sciences*, Vol. 18, April 1952, p. 287.

From the AIAA Progress in Astronautics and Aeronautics Series...

EXPERIMENTAL DIAGNOSTICS IN COMBUSTION OF SOLIDS—v. 63

Edited by Thomas L. Boggs, Naval Weapons Center, and Ben T. Zinn, Georgia Institute of Technology

The present volume was prepared as a sequel to Volume 53, *Experimental Diagnostics in Gas Phase Combustion Systems*, published in 1977. Its objective is similar to that of the gas phase combustion volume, namely, to assemble in one place a set of advanced expository treatments of diagnostic methods that have emerged in recent years in experimental combustion research in heterogenous systems and to analyze both the potentials and the shortcomings in ways that would suggest directions for future development. The emphasis in the first volume was on homogenous gas phase systems, usually the subject of idealized laboratory researches; the emphasis in the present volume is on heterogenous two- or more-phase systems typical of those encountered in practical combustors.

As remarked in the 1977 volume, the particular diagnostic methods selected for presentation were largely undeveloped a decade ago. However, these more powerful methods now make possible a deeper and much more detailed understanding of the complex processes in combustion than we had thought feasible at that time.

Like the previous one, this volume was planned as a means to disseminate the techniques hitherto known only to specialists to the much broader community of research scientists and development engineers in the combustion field. We believe that the articles and the selected references to the literature contained in the articles will prove useful and stimulating.

339 pp., 6 × 9, illus., including one four-color plate, \$20.00 Mem., \$35.00 List

TO ORDER WRITE: Publications Dept., AIAA, 1290 Avenue of the Americas, New York, N.Y. 10104